Effects of Electric Fields on Cathodoluminescence from II-VI Quantum Well Light Emitting Diodes

A. Y. Nikiforov,[1] G. S. Cargill III,[1] M. C. Tamargo,[2] S. P. Guo,[2,4] and Y.-C. Chen [3]

[1] Department of Materials Science and Engineering, Lehigh Univ., Bethlehem, PA 18015, U.S.A.
[2] Department of Chemistry, City College-CUNY, New York, NY 10031, U.S.A.
[3] Department of Physics, Hunter College, CUNY, New York, NY 10021, U.S.A.
[4] Present address: EMCORE Corp., Somerset, NJ 08873, U.S.A.

ABSTRACT

Effects of electrical bias on the cathodoluminescence (CL) have been investigated for a blue II-VI quantum well (QW) light emitting diode structure of ZnCdMgSe, lattice-matched to InP. In CL wavelength scans, the observed effects include largely reversible changes in QW CL intensity and wavelength and changes in cladding CL intensity. In CL time-based scans, the QW CL intensity showed both immediate and long term changes with bias. Irreversible, degradation-related decreases in QW CL intensity were also observed. Effects of bias on CL were modeled by calculating the rates of carrier production by electron bombardment and the resulting electron and hole currents with different applied bias fields. These model calculations do not explain many of the experimental observations, because the model does not include effects of bias on carrier escape and redistribution in the QW and effects of bias on generation and transport of atomic scale defects.

INTRODUCTION

ZnSe-based light emitting diodes have potential applications in full-color projection displays, traffic signals, and more efficient white light sources [1-5]. Although remarkable progress has been made, practical devices have not been yet achieved because of luminescent intensity degradation during device operation. The quaternary wide-gap ZnCdMgSe system (figure 1) can be grown lattice matched to (001) InP substrates by molecular beam epitaxy with a wide range of band gaps from blue to red depending on composition [3]. QW structures based on these materials exhibit excellent optical characteristics with very strong luminescence intensity and quantum confinement [4-5]. These diodes show no formation of dark line defects and have lifetimes about three orders of magnitude longer [6,7] than diodes with a comparable density of extended defects grown on GaAs substrates.

Understanding how electrical bias affects carrier transport and defect behavior may help in further improvement of performance and lifetimes of QW-based light emitting diodes (LEDs) and laser diodes [8]. Gundel et al. [8] studied the influence of reverse bias on degradation of a ZnCdSe QW-based laser diode by photoluminescence. They [8] argued that the observed changes in the degradation rate with bias were caused by the effects of bias fields on diffusion of charged defect complexes from the p-doped waveguide into the QW.
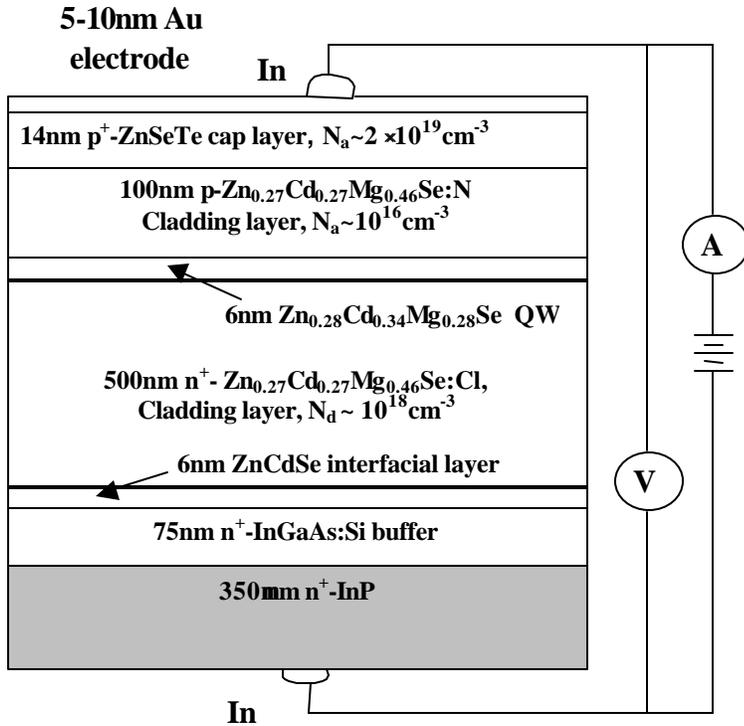
5-10nm Au electrode

In

| 14nm p^+-ZnSeTe cap layer, $N_a \sim 2 \times 10^{19} cm^{-3}$ |
| 100nm p-$Zn_{0.27}Cd_{0.27}Mg_{0.46}$Se:N Cladding layer, $N_a \sim 10^{16} cm^{-3}$ |
| 6nm $Zn_{0.28}Cd_{0.34}Mg_{0.28}$Se QW |
| 500nm n^+- $Zn_{0.27}Cd_{0.27}Mg_{0.46}$Se:Cl, Cladding layer, $N_d \sim 10^{18} cm^{-3}$ |
| 6nm ZnCdSe interfacial layer |
| 75nm n^+-InGaAs:Si buffer |
| 350mm n^+-InP |

In

Figure 1. Schematic of ZnCdMgSe QW-based LED and experimental setup.
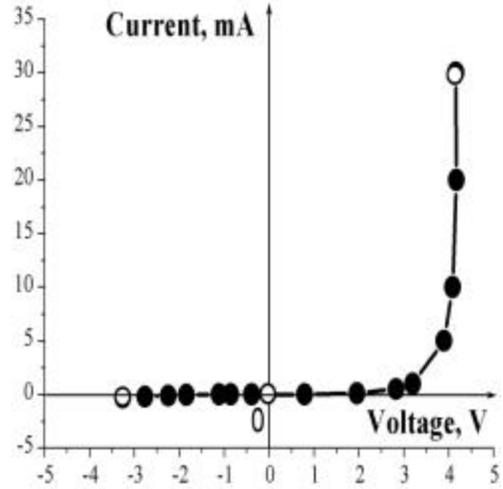
Figure 2. I-V characteristics of ZnCdMgSe QW-based LED. Open circles are bias conditions for CL experiments.

The present paper describes effects of both forward and reverse bias on CL from a ZnCdMgSe QW-based LED. Results obtained are much more extensive than those reported by Gundel et al. [8].

OBSERVED EFFECTS OF BIAS ON CATHODOLUMINESCENCE

CL measurements used a JEOL JSM-6400 SEM with an Oxford Instruments CF302 CL system. CL was studied for three biases: reverse bias of -3.2V, zero-bias, and forward bias of +4.2V, as indicated in figure 2. The electron beam voltage was 10kV and the electron beam current was ~ 50nA.

Cathodoluminescence wavelength measurements

Each wavelength scan was collected from an area of ~ $35\mu m \times 35\mu m$ and took about 160sec. Without bias, CL wavelength scans show well resolved peaks from the QW and cladding (figures 3 and 4). Application of either forward or reverse bias causes the QW CL intensity to drop. A forward bias of +4.2V eliminates the cladding peak and shifts the QW peak to longer wavelength (figure 3). These effects appear to be fully reversible. With a reverse bias of –3.2V, the cladding peak remains unaffected and a small increase in QW CL wavelength is observed (figure 4). In contrast to forward bias, a small irreversible decrease in QW CL, but not in cladding CL, is seen after switching from reverse bias to zero bias.
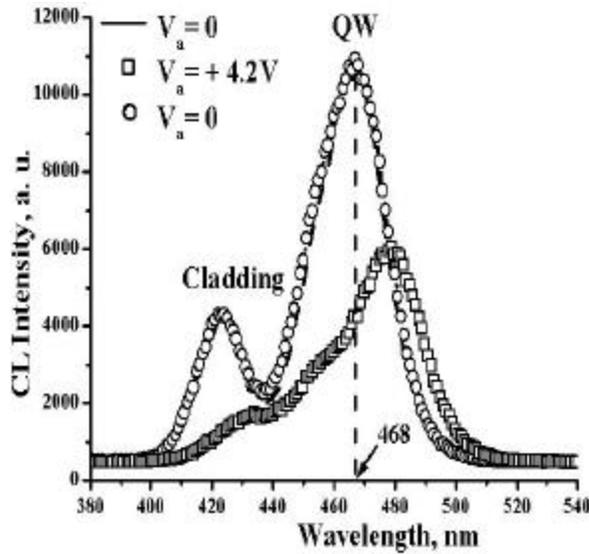
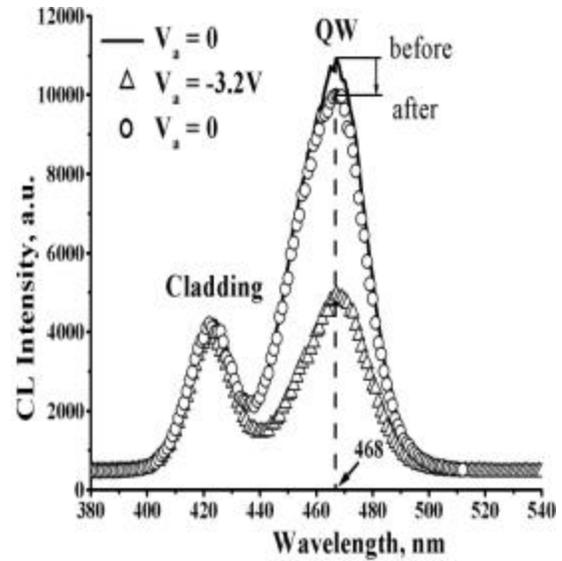**Figure 3**. Forward bias CL wavelength scans.
Figure 4. Reverse bias CL wavelength scans.

Time dependent effects of bias on quantum well cathodoluminescence

CL time-based scans were made with a stationary electron beam (spot mode) and with the spectrometer set to 468nm, the zero-bias QW CL wavelength. In the time-base scan without bias (figure 5), the QW intensity increased by ~10% during the initial 250s (A to B). Then the QW intensity remained nearly constant (B to C) until forward bias was applied. The decreases in the QW intensity to background level during the time-base scan, for example, at ~700s, resulted from blanking the electron beam. Forward bias led to a small, probably, instantaneous decrease (C to D), followed by a rapid decay of the QW intensity (D to F). When the bias was switched off (G), the QW intensity increased (G to H) to ~85% of its value before application of bias (C). Reverse bias caused the CL intensity to drop initially (H to I). The rate of the CL intensity decrease (I to K) for reverse bias was much slower than that for forward bias (D to F).
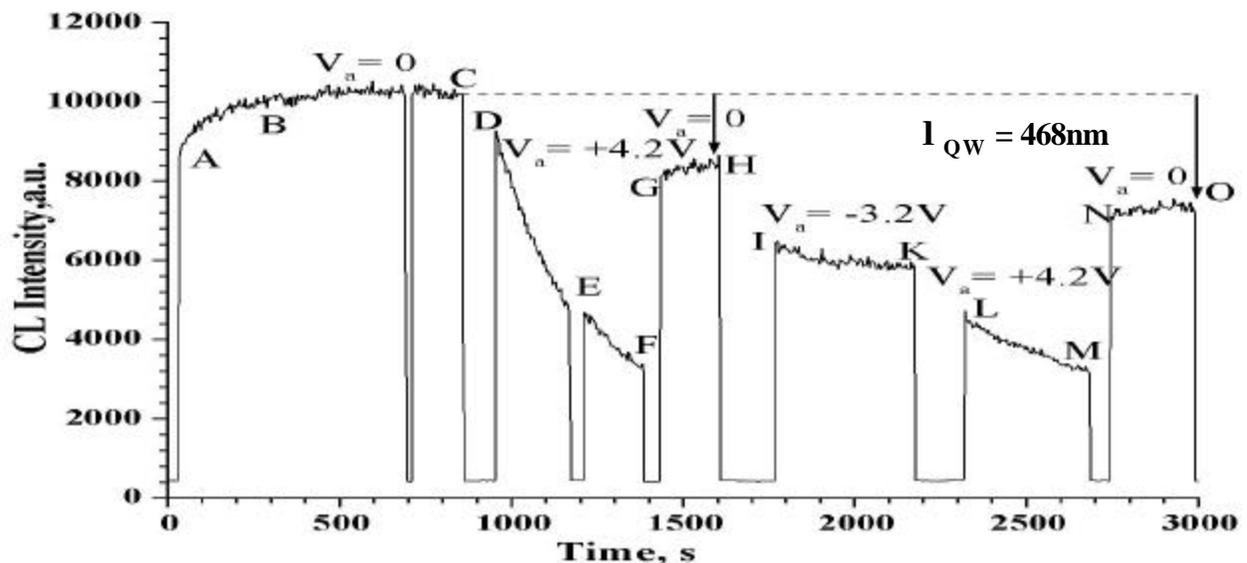

Figure 5. Bias effects in CL time-based scan. The arrows at 1600s and 3000s indicate zero-bias intensity decreases caused by electron bombardment.

Application of forward bias led to probably instantaneous QW intensity decrease (K to L) and further rapid intensity decay (L to M). After 3000s of spot mode electron irradiation with several biasing cycles, the QW intensity dropped by only ~30% (C to O). These bias effects are quite different from those reported by Gundel et al. [8] for a ZnCdSe QW-based laser diode, where rapid degradation occurred with zero bias.

MODELING EFFECTS OF BIAS ON CATHODOLUMINESCENCE FROM ZnCdMgSe QUANTUM WELL LIGHT EMITTING DIODES

Rates of electron and hole production by electron bombardment were calculated using the depth-distribution function (figure 6), which describes deposition of electron energy in depth. Effects of bias on band bending and depletion lengths were considered as well. Excess carriers, $\Delta n(\vec{r})$, generated in the specimen by continuous electron bombardment, undergo diffusion and/or drift, followed by recombination, that may give rise to luminescence. Assuming a linear dependence of CL intensity on the stationary excess carrier density, $\Delta n(\vec{r}) = n(\vec{r}) - n_0(\vec{r})$, the total CL intensity can be expressed as [9]

$$L_{CL}(\vec{r}) \propto \int_V \frac{\Delta n(\vec{r})}{t_{rr}} d^3 r ,$$ (1)

where t_{rr} is the radiative recombination lifetime.

Only excess carriers created by electron bombardment in the depletion regions, $W_{n,p}$, and within the diffusion length distances, $L_{n,p}$, (figures 6 and 7), contribute to the QW intensity. With reverse or zero bias, the depletion regions are much larger than the QW width, so diffusion and drift currents of excess minority carriers, I_{diff} and I_W, are expected to be largely responsible for the QW luminescence. The diffusion of the excess minority carriers, n_p and p_n, in one-dimension, can be treated in terms of the differential equations of continuity for electrons in the p-cladding and p^+-cap layers and for holes in the n-cladding layer (figure 1).

The local generation rate of excess carriers represents the number of electron-hole pairs generated per unit depth and per unit time [9]. This can be expressed as

$$g(z) = \frac{h(z) \times G \times I_b}{q} \left(\frac{\# \, pairs}{depth \times time} \right),$$ (2)

where $h(z)$ with $\int_0^\infty h(z)dz = 1$ is the depth-distribution of the deposited energy as a function of depth,
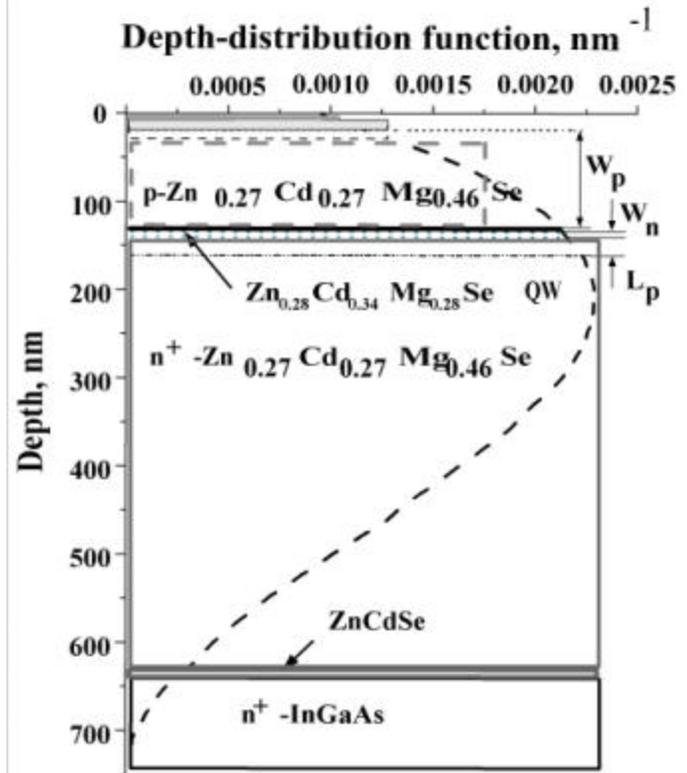

Figure 6. Depth-distribution function for ZnCdMgSe QW LED structure for 10kV electrons.

I_b is the electron beam current, and q is the electronic charge. G is the number of electron-hole pairs generated per incident electron of energy E_b,

$$G = \frac{E_b \times (1-g)}{E_i}, \qquad (3)$$

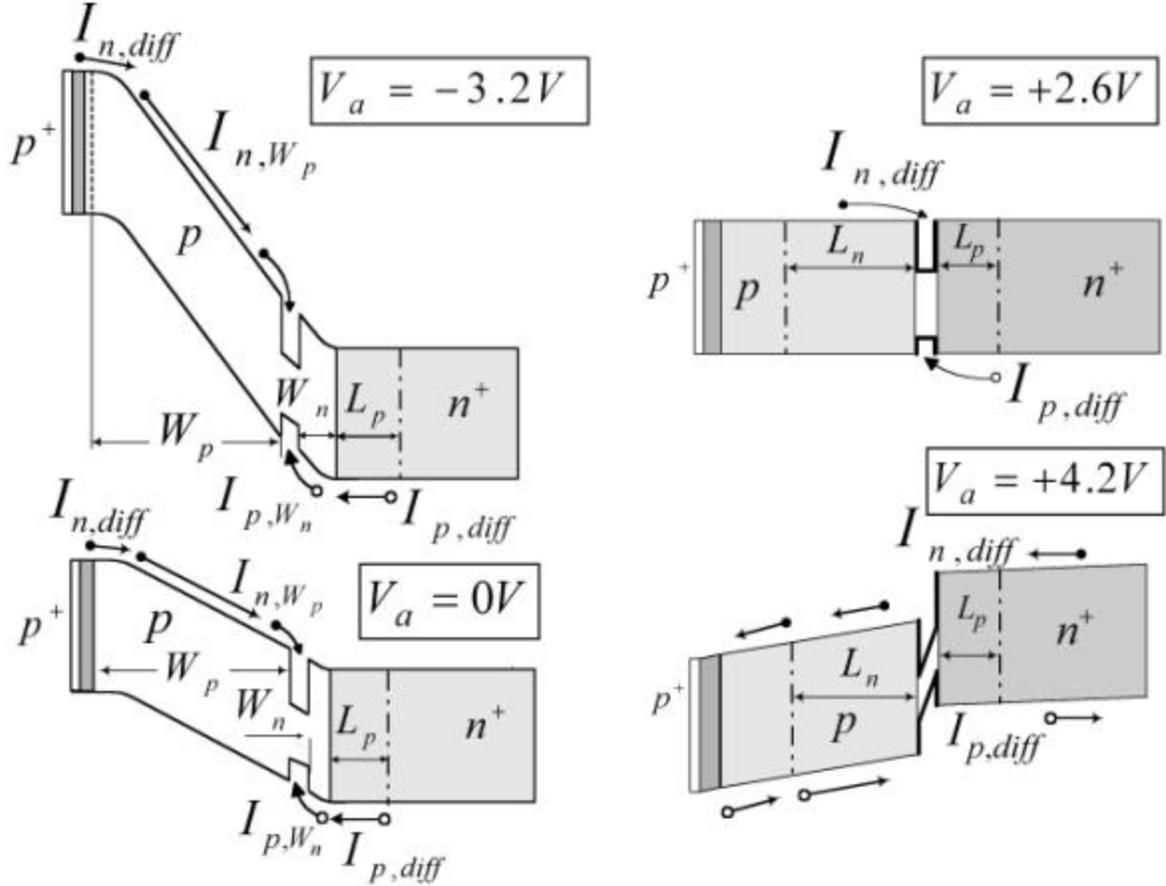**Figure 7.** Illustration of electric-field-induced band bending in QW LED structure.

where g is the fraction of electron beam energy loss due to backscattered electrons and E_i is the energy to form an electron-hole pair. Calculations of depth-distribution function (figure 6) and of minority carrier currents with and without bias were performed using structural and electrical parameters shown in figure 1. For regions W_p, W_n, L_p and L_n, the depth-distribution function was assumed to have its averaged value within each layer, as illustrated for the W_p region in figure 6. The bias dependence of drift currents enters through bias dependence of depletion widths, $W_{p,n}$, and of band bending, as shown schematically in figure 7.

Results of these calculations for bias voltages $V_a \leq 2.6$V, presented in figure 8, show that the electron current due to excess electrons excited by electron bombardment in the p-cladding layer and entering the QW is much larger than the hole current into the QW resulting from excess holes in the n-cladding layer excited by electron irradiation. This indicates that the resulting CL is a hole-limited process and should be proportional to the hole current. The calculations also indicate that luminescence should increase with reverse bias and decrease with forward bias. However, the luminescence intensity was experimentally observed to decrease with application of either forward or reverse bias (figures 3 and 4).
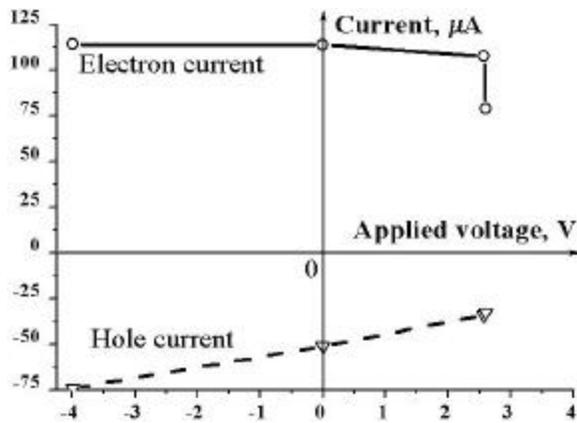
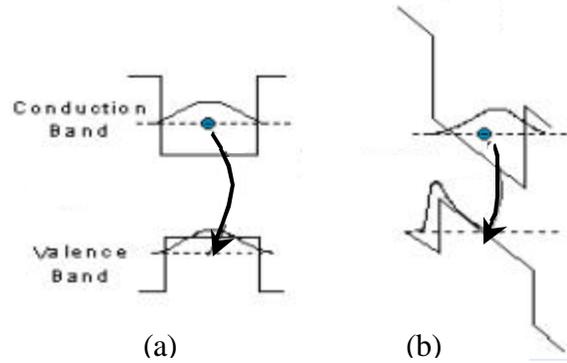**Figure 8.** Minority carrier currents into the ZnCdMgSe QW.

Figure 9. Expected effect of electric field on QW energy levels and wavefunctions, (a) zero field, (b) with applied field.

CONCLUSIONS

The present model does not explain many experimental observations, because it does not include forward bias levels beyond flat-band condition ($V_a \geq 2.6$V), and because it neglects effects of bias on carrier escape and redistribution in the QW (figure 9) [10]. The latter may be largely responsible for the reverse and forward bias QW CL intensity decrease and the forward bias QW CL redshift. Further CL experiments for intermediate biases, including flat-band condition, are needed to address these questions. To explain time-dependent QW CL intensity decreases and role of bias in degradation, the generation and transport of atomic scale defects must also be included in the model.

ACKNOWLEDGMENTS

REFERENCES

1. S. Itoh, K. Nakano, and A. Ishibashi, J. Cryst.Growth **214/215**, 1029 (2000).
2. A. Ishibashi, IEEE J. Select. Topics Quant. Electron. **1,** 741 (1995).
3. M. C. Tamargo, W. Lin, S. P. Guo, Y. Guo, Y. Luo, Y. C. Chen, J. Cryst. Growth **214/215** 1058 (2000).
4. M. C. Tamargo, S. P. Guo, O. Maksimov, Y. C. Chen, F. Peiris, and J. K. Furdyna, J. Cryst. Growth **227/228** 710 (2001).
5. S. P. Guo, L. Zeng, and M. C. Tamargo, Appl. Phys. Lett. **78**, 1957 (2001).
6. W. Faschinger and J. Nürnberger, Appl. Phys. Lett. **77**, 187 (2000).
7. D. Albert, J. Nurnberger, V. Hock, M. Ehinger, W. Faschinger, and G. Landwehr, Appl. Phys. Lett. **74**, 1957 (1999).
8. S. Gundel, D. Albert, J. Nurnberger, and W. Faschinger, Phys. Rev. B **60**, R16271 (1999); J. Cryst. Growth **214/215**, 474 (2000).
9. G. Yacobi and D. B. Holt, *Cathodoluminescence Microscopy of Inorganic Solids* (Plenum, 1990).
10. G. Bastard, *Wave Mechanics Applied to Semiconductor Heterostructures* (Les Editiones de Physique, Les Ulis, 1988).